Chinese Chemical Letters 35 (2024) 109757

Contents lists available at ScienceDirect

Chinese Chemical Letters

journal homepage: www.elsevier.com/locate/cclet

Supramolecular confinement effect enabling light-harvesting system for photocatalytic α-oxyamination reaction

Xuanyu Wang[1], Zhao Gao[1,*], Wei Tian[*]

Shaanxi Key Laboratory of Macromolecular Science and Technology, Xi'an Key Laboratory of Hybrid Luminescent Materials and Photonic Device, MOE Key Laboratory of Material Physics and Chemistry under Extraordinary Conditions, School of Chemistry and Chemical Engineering, Northwestern Polytechnical University, Xi'an 710072, China

ARTICLE INFO

Article history:
Received 3 January 2024
Revised 27 February 2024
Accepted 8 March 2024
Available online 16 March 2024

Keywords:
Self-assembly
Supramolecular chemistry
Light harvesting
Energy transfer
Confinement effect

ABSTRACT

The supramolecular Förster resonance energy transfer (FRET) is seen as a promising approach for organic photocatalysis using dyes as catalysts, because it combines the high efficiency of energy transfer with the dynamic responsiveness based on non-covalent interactions. Here we propose a supramolecular FRET photocatalysis strategy for α-oxyamination reaction based on supramolecular confinement effect. The well-designed benzothiadiazole-based cationic monomer as energy donor and the dyes of Nile Red as acceptor are doped into the amphiphilic surfactants of sodium dodecyl sulfate (SDS). Benefitting from the supramolecular confinement space provided by SDS in aqueous environment, the FRET process between the monomer and Nile Red is effectively achieved (exciton migration rate: 3.99×10^{14} L mol^{-1} s^{-1}). On this basis, the supramolecular FRET system is used as an efficient energy source to catalyze α-oxyamination reactions between a series of 1,3-dicarbonyl compounds and 2,2,6,6-tetramethylpiperidine-1-oxyl under white LED light, showing a yield as high as 94% and a turnover frequency value of 3.92 h^{-1}. This photocatalytic result shows a great enhancement compared to that of Nile Red alone.

Over the past decade, extensive research has been conducted in the realm of organic synthesis, with a particular focus on photocatalysis. This interest arises from the robust reactivity exhibited by many organic catalysts, enabling the facilitation of unique chemical reactions [1–4]. Typically, UV light serves as the excitation source for most reactions [5]. However, the utilization of this short-wavelength light not only results in the formation of by-products but also poses potential harm to human health. To address these concerns, organic dyes have emerged as promising alternatives for photocatalysts. Organic dyes, as photocatalysts, offer distinct advantages. Their excitation range falls within the visible region, enabling them to catalyze reactions under milder conditions. Moreover, they present benefits in terms of synthesis, scalability, ease of handling, and the capacity to choose from a broad spectrum of organic compounds to finely adjust electronic and photophysical properties [6–9]. Despite these advantages, traditional dyes like eosin Y and bengal rose red encounter challenges in altering molecular structures, thus limiting the facile adjustment of the redox potential of the photocatalyst to suit different substrates [10]. This limitation significantly constrains the advancement of dyes in the domain of organic photoredox catalysis.

To address this challenge, various approaches have been proposed to modify organic dyes, including the incorporation of transition metal complexes [11–13] and the development of heterogeneous catalysts [14–16]. However, these methods suffer from inefficiency to harvest the broadband light source and are often accompanied by adverse aggregation-caused quenching (ACQ) effect. As an alternative, the supramolecular Förster resonance energy transfer (FRET) system emerges as a promising avenue. This approach capitalizes on the combination of high energy transfer efficiency and dynamic responsiveness facilitated by non-covalent bonds [17–27]. By incorporating acceptors of organic dyes into the donors of supramolecular assemblies, thereby enabling the energy transfer process, the ACQ effect can be significantly mitigated, leading to an enhancement in photocatalytic efficiency. Several instances of supramolecular FRET catalysis have been reported by Wang's [28] and Zhang's [29] groups, wherein the non-covalent bonds predominantly focused on host-guest interactions. Nevertheless, the utilization of other types of supramolecular interactions to realize FRET photocatalysis is not yet clear and needs to be developed, as

* Corresponding authors.
E-mail addresses: gaozhao@nwpu.edu.cn (Z. Gao), happytw_3000@nwpu.edu.cn (W. Tian).
[1] These authors contributed equally to this work.

https://doi.org/10.1016/j.cclet.2024.109757
1001-8417/

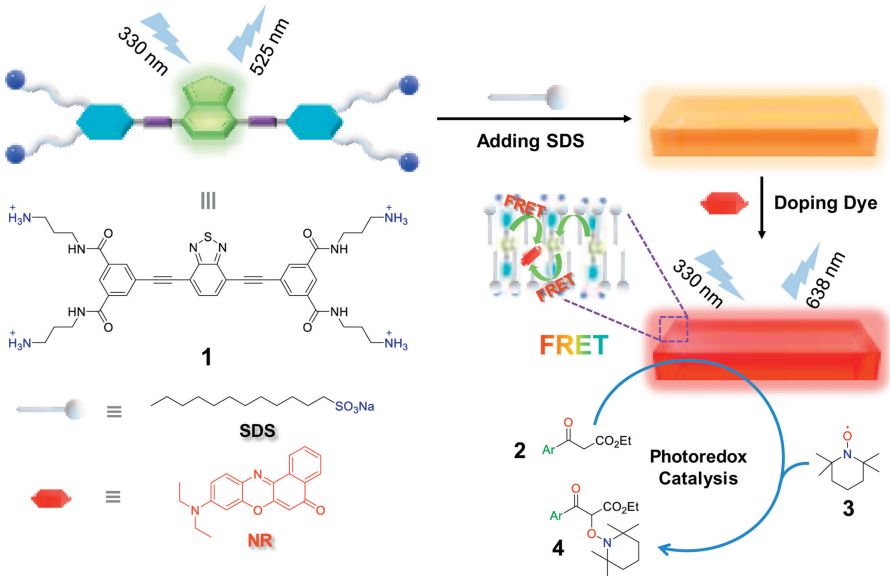

Fig. 1. Schematic illustration of light-harvesting systems and their application in photocatalytic reactions.

it is essential for the improvement of photocatalytic efficiency of dyes and the expansion of photocatalyst types.

The confinement effect, widely utilized as a constructional strategy due to its spatial selectivity and the ability to increase the number of active sites, finds extensive applications in organic synthesis [30,31] and optoelectronics [32,33]. Integrating the confinement effect into supramolecular FRET catalysis offers a dual advantage: not only does it bring the donor and acceptor into closer proximity, enhancing FRET efficiency, but it also positions the reactants closer to the catalyst center, thereby improving photocatalytic performance. Herein, we propose a supramolecular FRET photocatalysis strategy, in which the supramolecular confinement space is provided by the amphiphilic surfactants in an aqueous environment (Fig. 1). Specifically, a well-designed benzothiadiazole-based C_4-symmetric cationic monomer **1** is first synthesized, which dopes into the matrix of sodium dodecyl sulfate (SDS) surfactant to form the nanosheets of **1**/SDS. **1**/SDS acts as energy donor and reactor chamber. Upon the addition of the acceptor of Nile Red (NR) into **1**/SDS, an efficient light harvesting system **1**/SDS/NR is successfully established. On this basis, **1**/SDS/NR is employed as a photocatalyst for the α-oxyamination reaction between a series of 1,3-dicarbonyl compounds (**2**) and 2,2,6,6-tetramethylpiperidine-1-oxyl (TEMPO) (**3**) in an aqueous condition under white LED light. Comparative analysis with NR alone reveals a significant enhancement in photocatalytic activity for **1**/SDS/NR, achieving a yield as high as 94% and a turnover frequency (TOF) value of 3.92 h^{-1}. This marked improvement underscores the efficacy of the proposed supramolecular FRET photocatalysis strategy.

Spectroscopic experiments were first performed for the designed molecular **1**. In particular, its UV–vis spectrum showed two major absorption bands in diluted aqueous solution (1.5×10^{-5} mol/L, 303 and 405 nm, Fig. 2a, purple line). The fluorescence spectrum showed an emission band centered at 525 nm (absolute fluorescence quantum yield, $\Phi_F = 40.96\%$, Fig. 2a and Fig. S1 (Supporting information), which emitted a bright green-yellow color under excitation (Fig. 2a, inset). By plotting the emission of **1** against concentration, the critical aggregation concentration (CAC) was determined to be 3.89×10^{-5} mol/L (Fig. S2 in Supporting information) [34]. Despite the large spectral overlap integral (7.85×10^{15} nm^4 L mol^{-1} cm^{-1}) resulting from the absorption of NR in aqueous solution and the emission of **1**, indicating a potential for FRET to occur, the addition of NR to an aqueous solution of **1** did not induce the occurrence of the FRET process, even with an increased concentration above the CAC (Figs. S3 and S4 in Supporting information). This lack of FRET is attributed to the weak interactions between **1** and NR, making it challenging to form aggregates in water. Consequently, the distance between **1** and NR fails to meet the prerequisite conditions (<10 nm) for the occurrence of FRET [35].

To minimize the distance between **1** and NR, we chose SDS to provide confinement space for them. We first clarified the interaction between SDS and **1**. Upon gradually doping of **1** into SDS, the original absorption band of monomer **1** underwent a significant redshift, with three isosbestic points located at 312, 358 and 425 nm (Fig. S5a in Supporting information). Similarly, the emission band of **1** centered at 525 nm red-shifted to 550 nm and accompanied by a significant decrease in emission intensity ($\Phi_F = 4.40\%$, Figs. S5b and S1a in Supporting information). The morphologies of **1**/SDS observed by transmission electron microscopy revealed the formation of nanosheets (Fig. 3a). Additionally, the structure was confirmed through scanning electron microscopy and high-angle annular dark-field scanning transmission electron microscopy (Fig. S6 in Supporting information), along with energy-dispersive spectroscopy mapping (Fig. 3b). Moreover, the aqueous solution of **1**/SDS still maintained the same fluorescence emission after 48 days and its melting temperature obtained from the fitting was 320.51 K. These results proved that **1**/SDS was very stable in aqueous environment (Fig. S7 in Supporting information).

Subsequently, we investigated the FRET process between **1**/SDS and NR. Upon the gradual addition of NR to the aqueous solution of **1**/SDS, the intensity of the emission band centered at 550 nm for **1** gradually decreased, accompanied by a significant enhancement in the NR emission band centered at 638 nm ($\Phi_F = 5.07\%$, Fig. 2b and Fig. S1b in Supporting information). The CIE coordinates revealed a change in emission color from yellow to red (Fig. 2b inset and Fig. S8 in Supporting information). Notably, NR alone exhibited barely observable emission bands at the same concentration (Fig. S9c in Supporting information). Further insights into the FRET behaviors between **1**/SDS and NR were elucidated using two-dimensional excitation spectra (Fig. 2c). Excitation within the range of 300–450 nm led to a decline in the emission of donor **1**/SDS situated at 475–600 nm, while the emission signals of acceptor NR at 613–700 nm exhibited a significant enhancement. The spectral overlap integral of **1**/SDS with NR was calculated to be

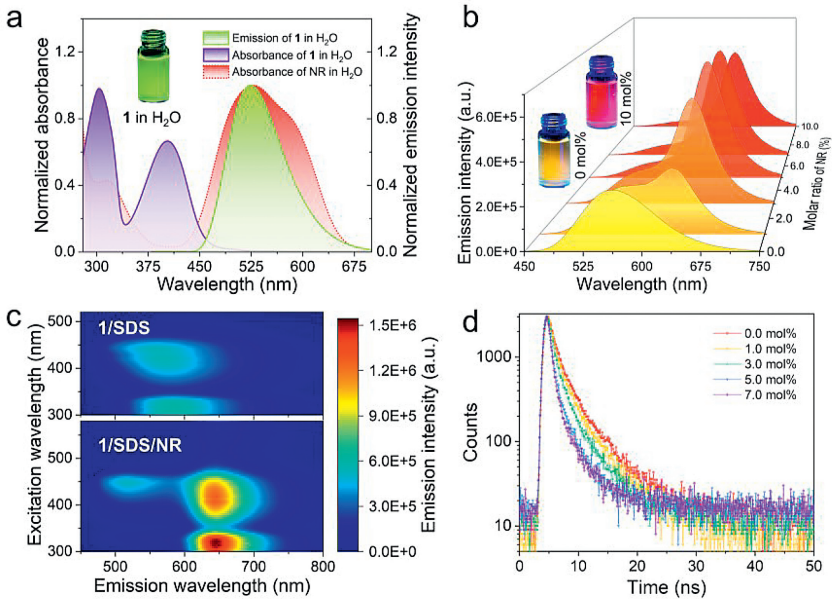

Fig. 2. Photophysical properties of monomers **1** and **1**/SDS/NR. (a) Normalized UV–vis absorption spectra of **1** and NR, and fluorescence spectra of **1** in water. Inset: the photograph of **1** in H_2O under 365 nm excitation. (b) Steady-state fluorescent spectra changes of **1**/SDS upon increasing the molar ratio of NR. Inset: the photograph of **1**/SDS at different concentrations of NR under 365 nm excitation. (c) Two-dimensional excitation spectra of the **1**/SDS and **1**/SDS/NR (10 mol% of NR). (d) Fluorescence lifetime decay profiles of **1**/SDS upon increasing the molar ratio of NR. All the concentrations of **1** and SDS were fixed at 1.5×10^{-5} mol/L and 1.8×10^{-4} mol/L, respectively.

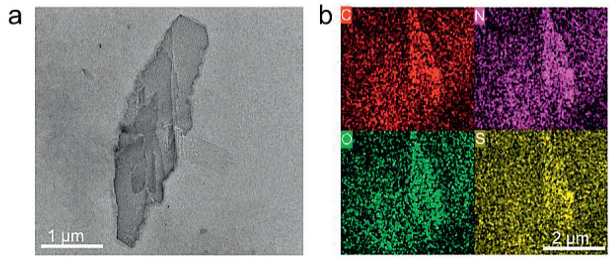

Fig. 3. Morphological studies for **1**/SDS. (a) TEM and (b) EDS images of different sample parts. The sample was obtained by slowly evaporating the aqueous solution of **1**/SDS ([**1**] = 3.0×10^{-5} mol/L, [SDS] = 3.6×10^{-4} mol/L).

4.02×10^{15} nm^4 L mol^{-1} cm^{-1} (Fig. S9a in Supporting information). This clearly indicated that the FRET behaviors could be well proceeded from **1**/SDS to NR. Similarly, for other confiment matrixes such as sodium dodecylbenzene sulfonate (SDBS) and sodium dodecyl sulfonate (AS), the FRET process between **1** and NR can be induced as well (Fig. S10 in Supporting information).

The mechanism of the FRET process was further elaborated. As the molar ratio of NR increased, the fluorescence lifetime (τ) of **1**/SDS decreased gradually (from 3.62 ns to 1.50 ns, Fig. 2d). In addition, the ratio plot of **1**/SDS/NR (I_{638nm}/I_{550nm}) increased linearly as the NR molar ratio changed from 0.0 to 10.0 mol%, suggesting that the acceptor was dispersed individually into the matrix of **1**/SDS (Fig. S9b in Supporting information). The ratio plot reached a plateau at higher NR concentration, suggesting that the dye had a tendency to form cluster in the **1**/SDS matrix (Fig. S11 in Supporting information). Importantly, based on the Fröster mechanism, the energy transfer efficiency and antenna effect were calculated to be 86.0% and 12.0, respectively (Fig. S9d in Supporting information). Furthermore, the *Stern-Volmer* plots of the average τ values and steady-state fluorescence intensity of **1**/SDS did not overlap at higher NR concentrations, which was characteristic of the fluorescence quenching of **1**/SDS comprising both dynamic and static quenching (Figs. S12a and b in Supporting information) [36]. Indeed, the calculated quenching efficiencies were dominated by the dynamic quenching efficiency (η_{dyn}) at low acceptor concentrations, while at high concentrations the η_{dyn} and static quenching efficiency (η_{stat}) were close to each other during the FRET process (Table S1 in Supporting information). We then determined the number of donors quenched by a single acceptor (n) using a mathematical model [37–40]. By plotting donor emission intensity versus acceptor concentration, a nonlinear curve fitting yielded a value of n of 19, suggesting a moderate quenching effect of acceptors on donors (Fig. S12c in Supporting information). Coulombic homo-transfer was used here to illustrate excitation energy delocalization in **1**/SDS/NR, which occurred as exciton diffusion [41–43]. By plotting $1/\tau$ of **1**/SDS against the concentration of NR, the second-order exciton migration rate for NR was calculated to be 3.99×10^{14} L mol^{-1} s^{-1}, which represents a large value of the FRET from **1**/SDS to NR (Fig. S12d in Supporting information). All these results manifested that we have successfully constructed an efficient FRET system of **1**/SDS/NR in aqueous solution.

Since efficient FRET system can be used as an energy source, we then dedicated to exploring the potential of **1**/SDS/NR in organic photocatalysis. The α-oxyamination reaction was selected, which is a useful transformation in organic synthesis [44,45]. Here we first performed this reaction between ethyl 3-oxo-3-phenylpropanoate (**2a**) and the free radical TEMPO (**3**) under visible light in aqueous medium. It can be clearly seen in Table 1, the yield of **4a** was dramatically increased when using the FRET system as a photocatalyst compared to NR alone. In entry 1, the yield of **4a** reached a maximum of 94% with a TOF value of 3.92 h^{-1} (Fig. S13 in Supporting information). As a comparison, there was no product generation when NR was used alone (Table 1, entry 3), and its catalytic activity was hardly observed (Fig. S14 in Supporting information). However, when the FRET catalytic system was placed in a dark environment, no products were generated (Table 1, entry 2), suggesting the importance of visible light in the catalytic cycle (Fig. S15 in Supporting information). For the other control groups, if the photocatalytic systems of **1**/SDS/NR miss one element, the product of **4a** could not be efficiently obtained (Table 1, entries 4–9 and Figs. S16–S20 in Supporting information). Based on the above results, the photo-catalytic mechanism was then proposed. As shown in

Table 1
Visible light induced photo-catalysis by FRET system.[a]

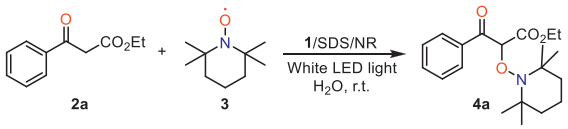

Entry	**1**/SDS (mol%)	NR (mol%)	Yields of **4a** (%) [b]	TOF (h^{-1})
1	7.5	1.5	94	3.92
2	7.5	1.5	n.r.[c]	0.00
3	None	1.5	n.r.	0.00
4	7.5	None	13	0.11
5	**1** (7.5 mol%)[d]	None	26	0.22
6	**1** (7.5 mol%)[d]	1.5	27	0.23
7	SDS (90.0 mol%)[e]	1.5	n.r.	0.00
8	SDS (90.0 mol%)[e]	None	n.r.	0.00
9	None	None	n.r.	0.00

[a] Reaction conditions: 3-oxo-3-phenylpropanoate **2a** (0.002 mmol), 2,2,6,6-tetramethylpiperidine-1-oxyl **3** (0.002 mmol), water (5 mL), stirring at room temperature.
[b] Crude yields determined from ^{1}H NRM based on the starting material with internal standard 1,3,5-trimethoxy benzene. Philips 40 W LED bulb (4000 Lm, 6500 K) has been used as visible light source.
[c] The reaction was performed in dark.
[d] Only **1** was used in the **1**/SDS system.
[e] Only SDS was used in the **1**/SDS system.

Table 2
Photo-catalysis by FRET system with different substrates.[a]

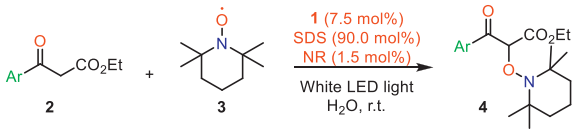

Entry	Ar	Product (**4**)	Yields (%)[b]	TOF (h^{-1})
1	4-OMe-Ph (**2b**)	**4b**	90	3.00
2	4-F-Ph (**2c**)	**4c**	86	4.41
3	4-Cl-Ph (**2d**)	**4d**	92	4.72
4	4-Br-Ph (**2e**)	**4e**	73	3.74
5	4-NO_2-Ph (**2f**)	**4f**	64	8.53

[a] Reaction conditions: 1,3-dicarbonyl **4** (0.002 mmol), 2,2,6,6-tetramethylpiperidine-1-oxyl **3** (0.002 mmol), water (5 mL), stirring at room temperature.
[b] Crude yields determined from ^{1}H NMR based on the starting material with internal standard 1,3,5-trimethoxy benzene.

Fig. S26 (Supporting information), upon photoexcitation with visible light, **1**/SDS transfers the energy to NR to form NR*. Then, as a reductant, it transferred an electron to substrate **2** through a single electron transfer process (SET). NR was recycled from the intermediate **5b** through another SET process. Finally, radical **5c** coupled with radical TEMPO to form product **4**.

Next, the scope of **1**/SDS/NR as photocatalyst was explored using a series of substrates **2**. As shown in Table 2, for all types of **2** with the electron-donating and electron-withdrawing groups, the α-oxyamination reaction could well proceed. Specifically, electron-donating groups resulted in an increase in reaction time (Table 2, entry 1 and Fig. S21 in Supporting information, TOF = 3.00 h^{-1} for **4b** *versus* 3.92 h^{-1} for **4a**). The halogen substituents of **2** exhibited a similar photocatalytic result compared to **2a** (Table 2, entries 2–4 and Figs. S21–S24 in Supporting information). In contrast, strong electron-withdrawing groups significantly shortened the reaction time but with a relatively low yield (Table 2, entry 5 and Fig. S25 in Supporting information). This may be attributed to the decomposition of the unstable product according to the literature [46]. All these results clearly indicate that we have successfully constructed a FRET system with great ability to catalyze organic reactions in water with visible light sources.

In summary, we have successfully established a supramolecular FRET photocatalytic system for α-oxyamination reaction. Benefiting from the supramolecular confinement effect induced by SDS, the FRET process between **1**/SDS and NR can be efficiently achieved. More importantly, the FRET system was used as an energy source to catalyze the α-oxyamination reaction under visible light in an aqueous solution, giving a significantly improved yield of 94% compared to NR alone. This work not only represents a general approach to construct supramolecular FRET systems, but also opens up a new avenue to organic photocatalysis.

Declaration of competing interests

The authors declare that they have no known competing financial interests or personal relationships that could have appeared to influence the work reported in this paper.

Acknowledgments

This work was financially supported by the National Natural Science Foundation of China (Nos. 22371230, 22022107, 22001213, and 22071197), the Postdoctoral Science Foundation of China (Nos. 2023M732855, 2022TQ0258), and the Shaanxi Fundamental Science Research Project for Chemistry & Biology (No. 22JHQ020). We would like to thank the Analytical & Testing Centre of Northwestern Polytechnical University for TEM and SEM tests.

Supplementary materials

Supplementary material associated with this article can be found, in the online version, at doi:10.1016/j.cclet.2024.109757.

References

[1] M.A. Bryden, E. Zysman-Colman, Chem. Soc. Rev. 50 (2021) 7587–7680.
[2] N.Y. Huang, Y.T. Zheng, D. Chen, et al., Chem. Soc. Rev. 52 (2023) 7949–8004.
[3] J.L. Li, S.L. Yang, Q.S. Dai, et al., Chin. Chem. Lett. 34 (2023) 108271.
[4] K. Kwon, R.T. Simons, M. Nandakumar, et al., Chem. Rev. 122 (2022) 2353–2428.
[5] A. Gualandi, M. Anselmi, F. Calogero, et al., Org. Biomol. Chem. 19 (2021) 3527–3550.
[6] N.A. Romero, D.A. Nicewicz, Chem. Rev. 116 (2016) 10075–10166.
[7] M. Neumann, S. Füldner, B. König, et al., Angew. Chem. Int. Ed. 50 (2011) 951–954.
[8] A.K. Yadav, L.D.S. Yadav, Green Chem. 17 (2015) 3515–3520.
[9] J. Yu, L. Zhang, G. Yan, Adv. Synth. Catal. 354 (2012) 2625–2628.
[10] P. Rana, N. Singh, P. Majumdar, et al., Coordin. Chem. Rev. 470 (2022) 214698.
[11] K.C. Dissanayake, P.O. Ebukuyo, Y.J. Dhahir, et al., Chem. Commun. 55 (2019) 4973–4976.
[12] Y. Anai, K. Shichijo, M. Fujitsuka, et al., Chem. Commun. 56 (2020) 11945–11948.
[13] J. Malone, S. Klaine, C. Alcantar, et al., New J. Chem. 45 (2021) 4977–4985.
[14] Y. Zhou, Z. Zhou, Y. Li, et al., Catal. Commun. 64 (2015) 96–100.
[15] M. Liras, M. Iglesias, F. Sánchez, Macromolecules 49 (2016) 1666–1673.
[16] W. Li, W. Zhang, X. Dong, et al., J. Mater. Chem. 22 (2012) 17445–17448.
[17] A.J.P. Teunissen, C. Pérez-Medina, A. Meijerink, et al., Chem. Soc. Rev. 47 (2018) 7027–7044.
[18] Z. Gao, L. Shi, F. Yan, et al., Angew. Chem. Int. Ed. 62 (2023) e202302274.
[19] T. Xiao, X. Li, L. Zhang, et al., Chin. Chem. Lett. 35 (2024) 108618.
[20] Z. Gao, F. Yan, L. Shi, et al., Chem. Sci. 13 (2022) 7892–7899.
[21] K.X. Teng, Z.P. An, L.Y. Niu, et al., ACS Mater. Lett 6 (2024) 290–297.
[22] S. Guo, Y. Song, Y. He, et al., Angew. Chem. Int. Ed. 57 (2018) 3163–3167.
[23] P. Wang, X. Miao, Y. Meng, et al., ACS Appl. Mater. Interfaces 12 (2022) 22630–22639.
[24] Y. Sun, L. Jiang, Y. Chen, et al., Chin. Chem. Lett. 35 (2024) 108644.
[25] Z. Wu, H. Qian, X. Li, et al., Chin. Chem. Lett. 35 (2024) 108829.
[26] H. Qian, T. Xiao, R.B.P. Elmes, et al., Chin. Chem. Lett. 34 (2023) 108185.
[27] T. Xiao, H. Wu, G. Sun, et al., Chem. Commun. 56 (2020) 12021–12024.
[28] M. Hao, G. Sun, M. Zuo, et al., Angew. Chem. Int. Ed. 59 (2020) 10095–10100.
[29] Z. Zhang, Z. Zhao, Y. Hou, et al., Angew. Chem. Int. Ed. 58 (2019) 8862–8866.
[30] J. Li, H. Jin, Z. Shang, et al., Chin. Chem. Lett. 34 (2023) 107912.
[31] Y. Xue, S. Jiang, H. Zhong, et al., Angew. Chem. Int. Ed. 61 (2022) e202110766.
[32] W.C. Chen, M.H. Zheng, Y.L. Wu, et al., Chem. Eng. J. 480 (2024) 148314.
[33] X.L. Tao, M.C. Pan, X. Yang, et al., Chin. Chem. Lett. 33 (2022) 4803–4807.
[34] Z. Gao, S. Qiu, F. Yan, et al., Chem. Sci. 12 (2021) 10041–10047.
[35] Q. Ling, T. Cheng, S. Tan, et al., Chin. Chem. Lett. 31 (2020) 2884–2890.

[36] C. Giansante, C. Schäfer, G. Raffy, et al., J. Phys. Chem. C 116 (2012) 21706–21716.
[37] H.Q. Peng, Y.Z. Chen, Y. Zhao, et al., Angew. Chem. Int. Ed. 51 (2012) 2088–2092.
[38] Y. Liu, J. Jin, H. Deng, et al., Angew. Chem. Int. Ed. 55 (2016) 7952–7957.
[39] G. Chadha, Q.Z. Yang, Y. Zhao, Chem. Commun. 51 (2015) 12939–12942.
[40] Z. Li, Y. Han, F. Wang, Nat. Commun. 10 (2019) 3735.
[41] A. Del Guerzo, A.G.L. Olive, J. Reichwagen, et al., J. Am. Chem. Soc. 127 (2005) 17984–17985.
[42] S. Banerjee, R.K. Das, P. Terech, et al., J. Mater. Chem. C 1 (2013) 3305–3316.
[43] K.T. Wong, D.M. Bassani, NPG Asia Mater. 6 (2014) e116.
[44] M.P. Sibi, M. Hasegawa, J. Am. Chem. Soc. 129 (2007) 4124.
[45] N.N. Bui, X.H. Ho, S.I. Mho, et al., Eur. J. Org. Chem. (2009) 5309 2009.
[46] H. Liu, W. Feng, C.W. Kee, et al., Green Chem. 12 (2010) 953–956.